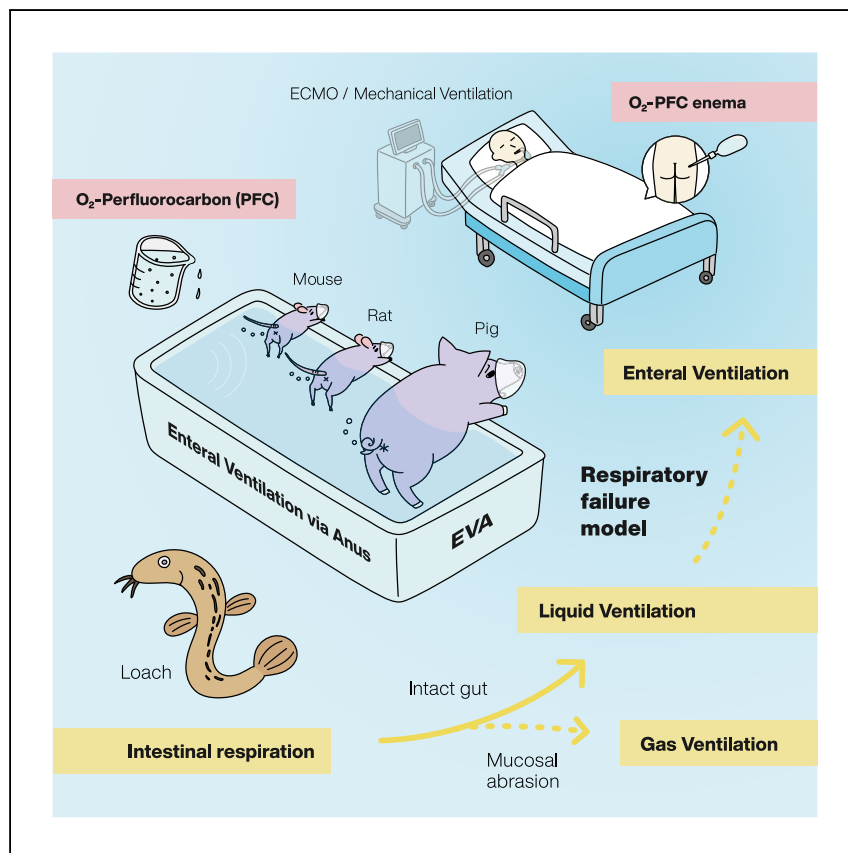


## Clinical and Translational Resource and Technology Insights

# Mammalian enteral ventilation ameliorates respiratory failure



Okabe et al. report the exploitation of intestinal breathing phenomenon in mammalian pre-clinical models, potentially offering an additional route of O<sub>2</sub> administration to patients who are in critical need of immediate respiratory support.

Ryo Okabe, Toyofumi F.  
Chen-Yoshikawa, Yosuke  
Yoneyama, ..., Eiji Kobayashi,  
Hiroshi Date, Takanori Takebe

takanori.takebe@cchmc.org

### Highlights

Enteral ventilation (EVA) enabled  
systemic oxygenation in  
mammalians

EVA improved survival and  
behaviors in pre-clinical models of  
respiratory failure

EVA yielded no major signs of  
complications in pre-clinical  
models

EVA may serve as a transformative  
approach in respiratory failure  
patients



## Pre-clinical Research

Okabe et al., Med 2, 773–783  
June 11, 2021 © 2021 Elsevier Inc.  
<https://doi.org/10.1016/j.medj.2021.04.004>



## Clinical and Translational Resource and Technology Insights

## Mammalian enteral ventilation ameliorates respiratory failure

Ryo Okabe,<sup>1,2</sup> Toyofumi F. Chen-Yoshikawa,<sup>3</sup> Yosuke Yoneyama,<sup>1</sup> Yuhei Yokoyama,<sup>2</sup> Satona Tanaka,<sup>2</sup> Akihiko Yoshizawa,<sup>4</sup> Wendy L. Thompson,<sup>5</sup> Gokul Kannan,<sup>6</sup> Eiji Kobayashi,<sup>7</sup> Hiroshi Date,<sup>2</sup> and Takanori Takebe<sup>1,5,7,8,9,10,\*</sup>

## SUMMARY

**Background:** Several aquatic organisms such as loaches have evolved unique intestinal breathing mechanisms to survive under extensive hypoxia. To date, it is highly controversial whether such capability can be adapted in mammalian species as another site for gas exchange. Here, we report the advent of the intestinal breathing phenomenon in mammals by exploiting EVA (enteral ventilation via anus).

**Methods:** Two different modes of EVA were investigated in an experimental model of respiratory failure: intra-rectal oxygen O<sub>2</sub> gas ventilation (g-EVA) or liquid ventilation (l-EVA) with oxygenated perfluorocarbon. After induction of type 1 respiratory failure, we analyzed the effectiveness of g-EVA and l-EVA in mouse and pig, followed by preclinical safety analysis in rat.

**Findings:** Both intra-rectal O<sub>2</sub> gas and oxygenated liquid delivery were shown to provide vital rescue of experimental models of respiratory failure, improving survival, behavior, and systemic O<sub>2</sub> level. A rodent and porcine model study confirmed the tolerable and repeatable features of an enema-like l-EVA procedure with no major signs of complications.

**Conclusions:** EVA has proven effective in mammals such that it oxygenated systemic circulation and ameliorated respiratory failure. Due to the proven safety of perfluorochemicals in clinics, EVA potentially provides an adjunctive means of oxygenation for patients under respiratory distress conditions.

**Funding:** This work is funded by the Research Program on Emerging and Re-emerging Infectious Diseases, Research Projects on COVID-19 (JP20fk0108278, 20fk0108506h0001), from the Japan Agency for Medical Research and Development (AMED), to T.T.; Strategic Promotion for Practical Application of Innovative Medical Technology, Seeds A (A145), to T.T.; and KAKENHI 19K22657, to T.C.-Y. This research is partially supported by the AMED Translational Research Program; Strategic Promotion for Practical Application of Innovative Medical Technology (TR-SPRINT), to T.C.-Y.; and AMED JP18bm0704025h0001 (Program for Technological Innovation of Regenerative Medicine), to T.T.

## INTRODUCTION

Improving hypoxia is the most important element to ameliorate respiratory failure. Notably, several unique non-mammalian species have evolved to adapt and survive under hypoxic environments by establishing accessory respiration mechanisms in organs other than lungs or gills. For example, loaches (*Misgurnus anguillicandatus*), sea cucumbers, *Corydoras*, and *Tetragnatha praedonia* use their posterior intestines for respiration.<sup>1–3</sup> Earlier studies in the 1950s and 1960s explored such mechanisms

## Context and significance

The SARS-CoV-2 pandemic has overwhelmed the clinical need for ventilators and artificial lungs, resulting in a critical shortage of available devices and endangering patients' lives worldwide. Inspired by organisms such as loaches that use intestinal air breathing, we show the effectiveness of an enteral ventilation approach in attaining systemic oxygenation in both rodent and porcine models. Intra-rectal delivery of a liquid form of O<sub>2</sub> known as conjugated perfluorocarbon, a compound historically used in clinics for liquid ventilation through airway administration, is highly tolerable and efficacious in ameliorating severe respiratory failure. Thus, by repurposing the distal gut as an accessory breathing organ, enteral ventilation therapy offers an alternative paradigm as an adjunctive means to patients who are in critical need of respiratory support.



in humans and animals yet with highly questionable outcomes regarding the breathing capabilities of mammalian digestive tracts mainly through the upper gastrointestinal (GI) organs.<sup>4–7</sup>

The mammalian rectum represents a body cavity covered by a relatively thin mucosal layer, particularly around the anal canal, in which abundant vascular drainage is made possible through hemorrhoidal plexuses connected both with the portal and the systemic circulation. Therefore, intra-anally administered drugs can be easily introduced and quickly absorbed around the rectal region.<sup>8</sup> Due to such anatomical features, we hypothesized that the mammalian distal gut enables efficient luminal access to submucosal blood vessels for potential gas exchange.

## RESULTS

In the loach, the posterior intestine is composed of a very thin epithelial layer, abundant capillary vessels, and erythrocytes,<sup>9</sup> which in environments of extensive hypoxia allow luminal access to oxygen (O<sub>2</sub>). To model this distal gut epithelium of the intestinal-breathing species, we attempted to abrade the mucosal barrier to allow for more efficient gas diffusion. First, chemical and mechanical thinning of epithelial layers were evaluated for their abilities to facilitate gas exchange via the distal gut. In doing so, we screened the protocols to best facilitate the oxygenation of venous outflow from the gut<sup>9</sup> (Table S1, groups 1–8; Figure 1B). Of these, a moderate mechanical abrasion protocol was the most efficient in permitting O<sub>2</sub> exchange with the gut lumen, with an increase of a  $13.6 \pm 5.66$ -mm Hg dissolved O<sub>2</sub> level compared to the non-abraded condition at the level of inferior vena cava (Figures 1A–1C). Quantitative RT-PCR analysis demonstrated that after moderate or severe abrasion, *Vegfa* and *Anxa1*, genes related to vascularization and mucosal inflammation, respectively, were significantly increased in the mouse gut, and also increased in the loach's gut (Figure S1A).<sup>9</sup> Thus, mucosal pre-conditioning by abrasion facilitates gas enteral ventilation via anus (g-EVA)-based gas exchange via the distal gut.<sup>10</sup>

The intestinal epithelial mucosa is an anaerobic environment, with PO<sub>2</sub> <10 mm Hg, and is responsive to hypoxic stimulation.<sup>10</sup> To further assess changes in local tissue hypoxia, the immunochemical staining of the gut with the Hypoxyprobe-1 kit was conducted in hypoxia-treated (FiO<sub>2</sub> 0.10) mice with or without g-EVA. In the absence of g-EVA, normal mice had positively stained cells (hypoxic cells) limited to the mucosal epithelium, whereas after hypoxia inhalation, the number of strongly positive cells increased and were distributed across the mucosal, submucosal, and connective tissues (Figures 1D, S1B, and S1C). In contrast, both in the non-abraded and the abraded g-EVA groups, there were fewer hypoxic cells (Figures 1D and S1C).

We further tested whether g-EVA has systemic oxygenation effects and thus has any therapeutic benefit. We evaluated the survival benefit of g-EVA against lethal hypoxia (FiO<sub>2</sub> 0.08; Table S1, groups 15–17). The control group had a 0% survival rate, with a median survival of <700 s (11 min). In contrast, g-EVA groups with intact gut showed a median survival of 1,127 s (18 min), whereas the abraded g-EVA group had a 75% survival rate at 50 min, which was statistically significant over controls ( $p < 0.001$ , Kaplan-Meier method and log-rank test; Figure 1E). The fatal manifestations such as cardiac arrest, the continuation of agonal respiration, and the arrest of mesenteric arterial pulse resolved in the abraded g-EVA group (Table S2). The partial pressure of O<sub>2</sub> in the inferior vena cava was

<sup>1</sup>Institute of Research, Tokyo Medical and Dental University (TMDU), 1-5-45 Yushima bunkyo-ku, Tokyo 113-8510, Japan

<sup>2</sup>Department of Thoracic Surgery, Graduate School of Medicine, Kyoto University, 54 Shogoin-Kawahara-cho, Sakyo-ku, Kyoto 606-8507, Japan

<sup>3</sup>Department of Thoracic Surgery, Graduate School of Medicine, Nagoya University, 65 Tsurumai-cho, Showa-ku, Nagoya 466-8550, Japan

<sup>4</sup>Department of Diagnostic Pathology, Kyoto University Hospital, 54 Shogoin-kawahara-cho, Sakyo-ku, Kyoto 606-8507, Japan

<sup>5</sup>Division of Gastroenterology, Hepatology & Nutrition, Developmental Biology, Center for Stem Cell and Organoid Medicine (CuSTOM). Cincinnati Children's Hospital Medical Center, 3333 Burnet Avenue, Cincinnati, OH 45229-3039, USA

<sup>6</sup>Department of Chemical and Biomolecular Engineering, University of California, Berkeley, Berkeley, CA 94720-1462, USA

<sup>7</sup>Department of Organ Fabrication, Keio University School of Medicine, Keio, 35 Shinanomachi, Shinjuku-ku, Tokyo 160-8582, Japan

<sup>8</sup>Department of Pediatrics, University of Cincinnati College of Medicine, 3333 Burnet Avenue, Cincinnati, OH 45229-3026, USA

<sup>9</sup>Communication Design Center, Advanced Medical Research Center, Yokohama City University Graduate School of Medicine, 3-9 Fukuura, Kanazawa-ku, Yokohama, Kanagawa 236-0004, Japan

<sup>10</sup>Lead contact

\*Correspondence: [takanori.takebe@cchmc.org](mailto:takanori.takebe@cchmc.org)  
<https://doi.org/10.1016/j.medj.2021.04.004>

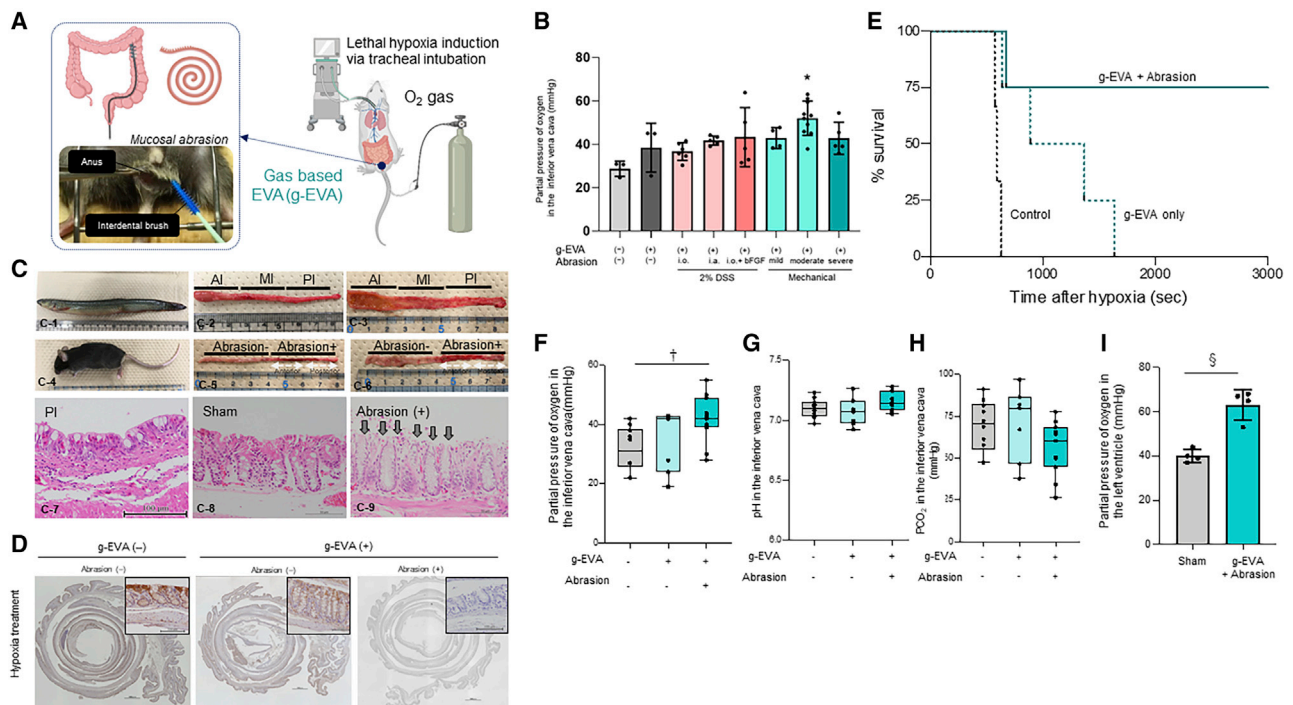


**Figure 1. O<sub>2</sub> gas-based enteral ventilation via anus (EVA) rescue lethal hypoxia by systemic oxygenation**

(A) Graphic visualization of intestinal gas ventilation (g-EVA) methods on the left. The figure on the right is an actual photo during surgery.

(B) Optimization of mucosal conditioning protocols for intestinal g-EVA based on partial venous pressure of O<sub>2</sub>. PvO<sub>2</sub> 52.0 ± 7.88 mm Hg and 38.4 ± 11.3 mm Hg,  $p = 0.042$ . Data of surviving mice only.

(C) Gross appearance and hematoxylin staining of the normal loach posterior intestine and mouse intestine with or without abrasion. (C-1) The gross appearance and (C-2) the intestinal appearance of a loach. AI, anterior intestine; MI, middle intestine; PI, posterior intestine. (C-3) The cross-sectional view of the intact intestine (C-4). The gross appearance and (C-5) the intestinal appearance of a mouse. (C-6) The cross-sectional view of the abraded intestine of a mouse. The hematoxylin staining of the posterior intestine of a loach (C-7), large intestine of a mouse (C-8), mechanical abraded large intestine of a mouse (C-9), and the loss of intestinal epithelial cells due to abrasion (C-9, red arrowhead).

(D) The immunochemical staining of Hypoxyprobe in the intestine under extensive hypoxia. The mouse intestine under severe hypoxia with abrasion and g-EVA showed a significant reduction of local tissue hypoxia.

(E) The survival rate under critical hypoxia.

(F) The improvement of oxygenation in the inferior vena cava with abraded g-EVA.  $^{\dagger}p < 0.01$ .

(G) The pH in the inferior vena cava.

(H) The pressure of carbonate dioxide in the inferior vena cava.

(I) The improvement of oxygenation in the left ventricle of the heart with abraded g-EVA.  $^{\S}p < 0.001$ .

statistically higher in the abraded g-EVA group than that in the sham group ( $p = 0.004$ ). The venous pressure levels of O<sub>2</sub> among sham, non-abraded g-EVA, and abraded g-EVA groups were 31.6 ± 7.44, 32.9 ± 10.6, and 40.3 ± 9.57 mm Hg, respectively (FiO<sub>2</sub> 0.21; Figure 1F). The venous pH, the venous pressure of carbon dioxide (CO<sub>2</sub>), and the concentration of base excess, bicarbonate ion, and lactate showed no significant difference among the sham, non-abraded g-EVA, and abraded g-EVA groups (Figures 1G, 1H, and S2A–S2C). Similarly, the partial arterial pressure of O<sub>2</sub> in the left ventricle of the heart under hypoxic inhalation was statistically higher in the abraded g-EVA group than that of the sham group ( $p = 0.030$ ). The pressure levels of O<sub>2</sub> between the sham and abraded g-EVA groups were 40.0 ± 2.94 and 63.3 ± 6.94 mm Hg, respectively (FiO<sub>2</sub> 0.10; Figure 1I). The pH and the partial pressure of CO<sub>2</sub> showed no statistically significant difference between the sham and abraded g-EVA groups (Figures S2D and S2E). Intestinal gas ventilation was effective for systemic oxygenation and in mitigating lethal hypoxia.

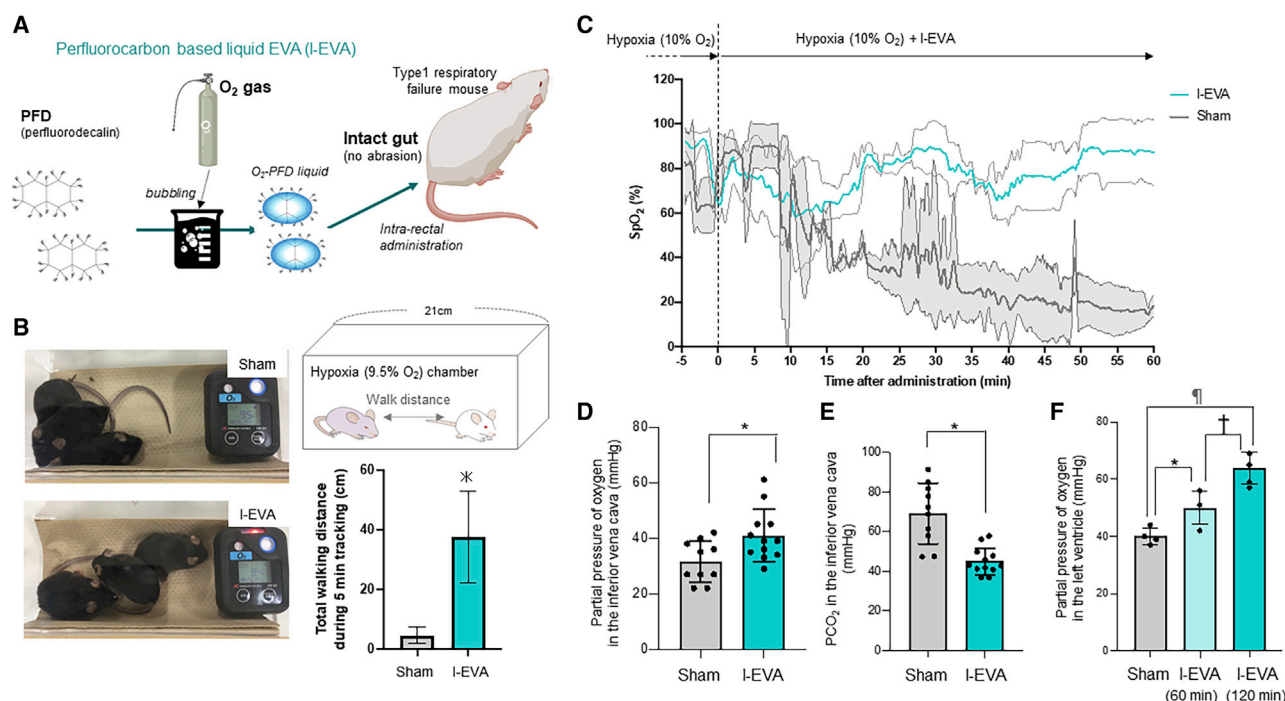


**Figure 2. O<sub>2</sub> loaded PFC-based EVA rescues lethal hypoxia with intact gut**

- (A) Schematic of the experimental procedure.  
 (B) Video tracking of the walking distances in intestinal liquid ventilation (I-EVA) group versus sham group, \* $p < 0.0001$ .  
 (C) The continuous monitoring of O<sub>2</sub> saturation by pulse oximetry in a mouse exposed to hypoxia.  
 (D) The improvement of oxygenation in the inferior vena cava with intestinal I-EVA, \* $p < 0.05$ .  
 (E) The pH in the inferior vena cava at 120 min.  
 (F) The pressure of carbon dioxide in the inferior vena cava, \* $p < 0.05$ .

Although gas-based EVA has been effective, particularly when abraded, it is unlikely to be clinically feasible, especially in severely ill patients. Alternatively, we approached an oxygenated perfluorodecalin (PFD), a liquid that has a remarkable adsorbing capacity for O<sub>2</sub> and CO<sub>2</sub> to devise liquid-based EVA (I-EVA). Due to its biocompatibility and safety in humans through intra-airway,<sup>11</sup> ocular,<sup>12</sup> and blood<sup>13</sup> infusion, intrapulmonary application of perfluorochemical in liquid or aerosol is already used in clinics to reduce lung injury in pediatric cases of severe respiratory insufficiency.<sup>11</sup> The low surface tension and high density allows perfluorocarbon to serve as surfactant substitutes.<sup>11,14</sup> The potential use of hydrophobic and lipophobic perfluorochemicals as inert carriers of O<sub>2</sub> via a rectal delivery method may offer several theoretical advantages over gas-based approaches.<sup>8</sup>

O<sub>2</sub>-loaded PFD was thus prepared (1L O<sub>2</sub> bubbling per minute for 45 min; Figure 2A) and the PFD liquid was subsequently infused via the rectum at a total volume of 1 mL per mouse, hereafter defined as the I-EVA group. The average O<sub>2</sub> pressure in the PFD was  $438 \pm 19.9$  mm Hg ( $n = 3$ ; Figure S2J). The therapeutic effect of I-EVA was assessed in a non-lethal respiratory failure mouse model in a 10% O<sub>2</sub> chamber (Method details). After hypoxia induction in the chamber, time-lapse video analysis showed clear symptomatic relief by I-EVA treatment (Video S2). The walking distance of each mouse was calculated and there was a significant increase in the O<sub>2</sub>-PFD liquid-injected group compared to the sham group in the hypoxic chamber (FiO<sub>2</sub> 0.10, sham group,  $0.408 \pm 1.02$  cm/20 s; FiO<sub>2</sub> 0.10, therapy group,  $3.34 \pm 4.05$  cm,  $p < 0.0001$ , Figure 2B). Next, continuous SpO<sub>2</sub> monitoring was applied



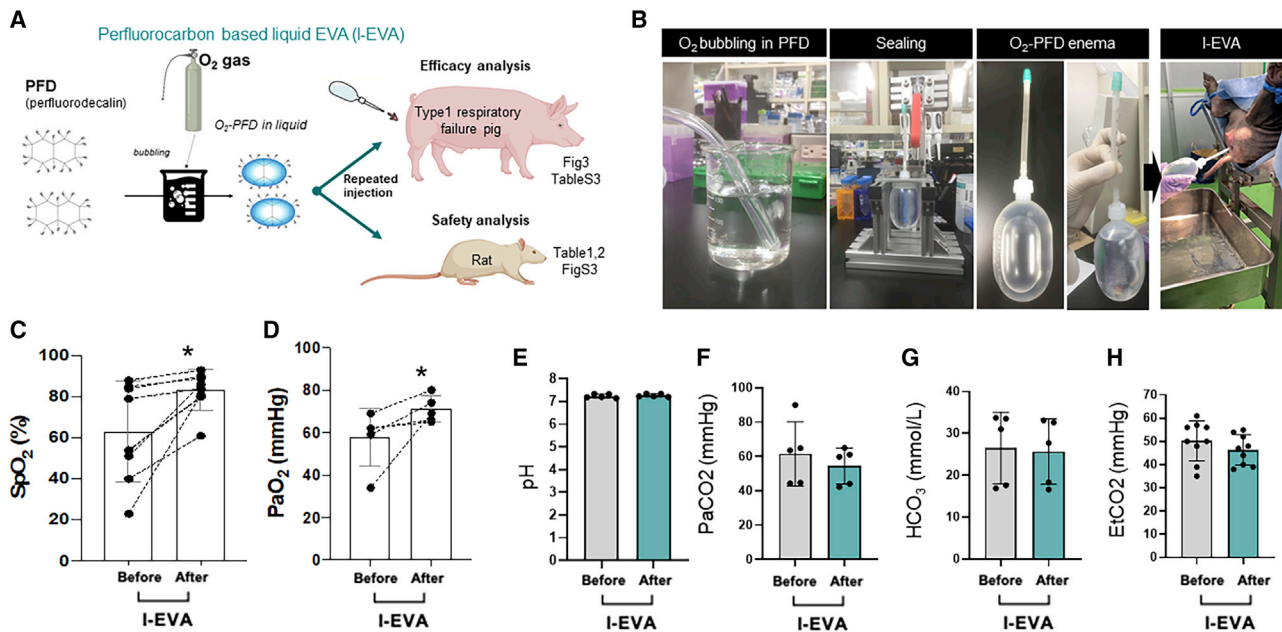


**Figure 3. I-EVA systemically and repeatedly oxygenates in porcine model of hypoxia**

(A) The surgical procedure for this experiment. PFD bubbled with pure O<sub>2</sub> for 30 min was administered into the rectums of pigs.

(B) I-EVA procedure. The PFD is bubbled with pure O<sub>2</sub>, filled in an enema container, and sealed. It is then administered into the rectum using the enema container.

(C and D) Repeated doses of PFD increased SpO<sub>2</sub> by 15% and PaO<sub>2</sub> by 13 mm Hg. \*p < 0.05.

(E–H) The partial arterial concentration of the pH, PaCO<sub>2</sub>, HCO<sub>3</sub><sup>-</sup>, and EtCO<sub>2</sub>.

to the mice under artificial ventilatory control at 10% hypoxia, demonstrating that the reversal of hypoxia was maintained for at least 60 min (Figure 2C). In the room air environment, the partial pressure of O<sub>2</sub> in the inferior vena cava was significantly higher in the I-EVA group than in the sham group (120 min,  $p = 0.037$ ) and the difference in pressures between these 2 groups was  $9.40 \pm 3.65$  mm Hg (Figure 2D). While the venous pH remained similar between the sham and I-EVA groups (Figure 2E), the venous pressure of CO<sub>2</sub>, the concentration of base excess bicarbonate ion showed decreasing trends ( $p < 0.0001$ ,  $p = 0.021$  and  $p = 0.001$ , respectively; Figures 2F, S2F, and S2G). The partial pressure of O<sub>2</sub> in the left ventricle of the heart was also significantly higher in the I-EVA group than in the control group 60 min after I-EVA (Figure S2H), with more pronounced differences in pressures ( $23.8 \pm 3.11$  mm Hg) observed between these 2 groups at 120 min,  $p = 0.020$ . The pH showed no statistically significant difference between these 2 groups at 120 min (Figure S2I). We next compared the partial pressure of O<sub>2</sub> in the ventricle of the heart after O<sub>2</sub>-PFD treatment with the I-EVA model. We found that the partial pressure of O<sub>2</sub> in the ventricle of the heart was equivalent between the g-EVA group and the I-EVA group under a hypoxic environment (g-EVA group; PaO<sub>2</sub>  $63.3 \pm 6.95$  mm Hg, I-EVA group; PaO<sub>2</sub>  $63.8 \pm 5.59$  mm Hg,  $p = 0.80$ ). These data suggest that rectal administration of O<sub>2</sub>-loaded PFD is sufficient to rescue oxygenation levels in a hypoxic mouse model in an intact gut.

To further assess the therapeutic potential of the enteral ventilation mechanism, we applied I-EVA under non-lethal conditions by hypoventilation (ventilatory rate: 5–6 times/min) in a large animal model (Method details). We performed SpO<sub>2</sub> and blood gas analysis following repeated intra-rectal O<sub>2</sub>-PFD administration in a pig model (Figures 3A and 3B). After 400 mL O<sub>2</sub>-PFD administration, the SpO<sub>2</sub> and PaO<sub>2</sub> levels

**Table 1. PFD concentration in whole blood by gas chromatography-mass spectrometry**

AnimalNo.	Time, h	Concentration ( $\mu\text{g/mL}$ )*
02M01	0.5	<LLOQ (0.320)
	2	<LLOQ (0.325)
	24	<LLOQ (0.197)
02M02	0.5	<LLOQ (N.D.)
	2	<LLOQ (0.254)
	24	<LLOQ (0.363)
02M03	0.5	<LLOQ (0.143)
	2	<LLOQ (0.242)
	24	<LLOQ (0.145)
03M01	0.5	<LLOQ (0.423)
	2	<LLOQ (0.460)
	24	<LLOQ (0.241)
03M02	0.5	<LLOQ (0.434)
	2	<LLOQ (0.434)
	24	<LLOQ (0.313)
03M03	0.5	<LLOQ (0.336)
	2	<LLOQ (0.290)
	24	<LLOQ (0.0678)

\*LLOQ, lower limit of quantitation (1  $\mu\text{g/mL}$ ).

have increased by 15% (from  $66.6\% \pm 24.1\%$  to  $81.8\% \pm 11.2\%$ ,  $p = 0.018$ ) and 13 mm Hg (from  $57.2 \pm 13.5$  to  $70.8 \pm 6.22$  mm Hg,  $p = 0.037$ ; [Figures 3C](#) and [3D](#)), while pH,  $\text{HCO}_3^-$ , and  $\text{EtCO}_2$  remain unchanged (pH:  $7.24 \pm 0.0837$  to  $7.27 \pm 0.0665$ ,  $p = 0.053$ ,  $\text{HCO}_3^-$ :  $26.5 \pm 8.55$  to  $25.7 \pm 7.81$ ,  $p = 0.13$ ;  $\text{EtCO}_2$ :  $50.2 \pm 8.60$  to  $46.3 \pm 6.50$  mm Hg,  $p = 0.053$ ; [Figures 3E](#), [3G](#), and [3H](#)).  $\text{PaCO}_2$ , by contrast, tended to decrease ( $\text{PaCO}_2$ :  $61.5 \pm 18.8$  to  $54.4 \pm 10.5$  mm Hg,  $p = 0.098$ ; [Figure 3F](#)). After removing the  $\text{O}_2$ -released PFD and re-administering  $\text{O}_2$ -PFD, the cycle was repeated periodically. The improvements of  $\text{SpO}_2$  and  $\text{PaO}_2$  in this repetitive cycle with  $\text{O}_2$ -PFD are consistent and reproducible ( $1.44 \pm 0.803$ - and  $1.31 \pm 0.410$ -fold increase over pre-treatment level, respectively, [Figures 3C](#) and [3D](#)). The mean persistence of  $\text{SpO}_2$  improvement ( $>5\%$ ) was  $18.7 \pm 2.31$  min per dose of  $\text{O}_2$ -PFD. Throughout the procedures, no obvious side effects were noted. Hypoxia-associated skin pallor and peripheral coldness resolved in the I-EVA group ([Table S3](#)). A proof-of-principle EVA approach is effective in providing  $\text{O}_2$  and alleviating respiratory failure symptoms in two mammalian model systems.

To further evaluate the safety features of I-EVA, we established PFD quantification methods in a rat model to determine any potential absorption of the infused chemicals. Gas chromatography-mass spectrometry analysis showed that serum PFD levels are below the lower limit of quantification (1  $\mu\text{g/mL}$ ), although a minor chromatographic peak was detected at almost all of the time points ([Table 1](#)). Physical examination revealed the absence of notable side effects such as diarrhea and dehydration. This is further supported by comprehensive laboratory testing at day 2 with extensive PFD infusion protocols (6 times infusion and 2 different doses; 1 and 1.5 mL/dose), revealing no abnormal elevation of each measured value, including hematocrit, albumin, and electrolytes ([Table 2](#)). Postmortem pathology analysis both in pig and rat after repeated I-EVA revealed the presence of intact gut, liver/bile duct, and spleen without cytoplasmic vacuolation of reticuloendothelial cells, which is a histopathological hallmark of systemic absorption and accumulation of PFD<sup>15</sup> ([Figures S3A](#) and [S3B](#)). The other organ toxicity markers such as aspartate aminotransferase (AST), alanine aminotransferase (ALT), glutamate dehydrogenase

**Table 2. Analysis of systemic toxicity by laboratory testing**

Substance	Saline	PFD	PFD	
Dose volume (mL/head)	1	1	1.5	
No. doses (time/day)	6	6	6	
Blood collection time	Day 2	Day 2	Day 2	p
Erythrocytes, $\times 10^4/\mu\text{L}$	778 $\pm$ 40	752 $\pm$ 24	791 $\pm$ 24	N.S.
Hematocrit, %	45.7 $\pm$ 2.4	45.0 $\pm$ 1.1	45.6 $\pm$ 1.4	N.S.
Hemoglobin, g/dL	15.3 $\pm$ 0.8	15.1 $\pm$ 0.7	15.2 $\pm$ 0.6	N.S.
Platelets, $10^4/\mu\text{L}$	103 $\pm$ 16.1	112 $\pm$ 11.5	123.5 $\pm$ 20.1	N.S.
Leukocytes, $10^2/\mu\text{L}$	82 $\pm$ 10	102 $\pm$ 18	88 $\pm$ 5	N.S.
Albumin, g/dL	2.6 $\pm$ 0.1	2.6 $\pm$ 0.1	2.6 $\pm$ 0.1	N.S.
Glucose, mg/dL	124 $\pm$ 7	123 $\pm$ 22	123 $\pm$ 18	N.S.
Total cholesterol, mg/dL	62 $\pm$ 10	75 $\pm$ 20	71 $\pm$ 22	N.S.
Triglyceride, mg/dL	25 $\pm$ 15	21 $\pm$ 7	20 $\pm$ 4	N.S.
Urea nitrogen, mg/dL	14 $\pm$ 2	14 $\pm$ 2	14 $\pm$ 2	N.S.
Creatinine, mg/dL	0.2 $\pm$ 0.1	0.2 $\pm$ 0.1	0.3 $\pm$ 0.1	N.S.
AST, U/L	108 $\pm$ 24	68 $\pm$ 2	72 $\pm$ 5	N.S.
ALT, U/L	31 $\pm$ 2	24 $\pm$ 3*	25 $\pm$ 1*	*p < 0.05
ALP, U/L	583 $\pm$ 135	470 $\pm$ 112	540 $\pm$ 64	N.S.
CK, U/L	162 $\pm$ 31	170 $\pm$ 22	196 $\pm$ 12	N.S.
Sodium, mmol/L	143 $\pm$ 1	143 $\pm$ 1	143 $\pm$ 1	N.S.
Potassium, mmol/L	3.4 $\pm$ 0.2	3.6 $\pm$ 0.2	3.6 $\pm$ 0.2	N.S.
Chloride, mmol/L	104 $\pm$ 1	103 $\pm$ 1	105 $\pm$ 1	N.S.
Calcium, mmol/L	10.2 $\pm$ 0.4	10.1 $\pm$ 0.1	9.9 $\pm$ 0.3	N.S.

ALP, alkaline phosphatase; AST, aspartate aminotransferase; CK, creatine kinase; N.S., not significant.

\*There was a statistically significant decrease in ALT in each PFD group compared to the saline group. However, this difference was significant due to the high levels in the saline group and was not considered a PFD-induced decrease.

(GLDH), alkaline phosphatase (ALP), and creatine kinase (CK) were comparable with or less than those of the saline control (Table 2). We also determined bacterial endotoxin (lipopolysaccharide [LPS]) levels in the serum and all of the measures were below the detection limit (<0.003 EU/mL) both in mice and pigs (Table 3), alleviating the concerns of bacterial translocation. Thus, I-EVA protocols do not cause obvious side effects, at least in the short term in our preclinical models.

## DISCUSSION

Inspired by aquatic organisms, we exploited intestinal ventilation mechanisms in multiple mammalian species. Collective evidence indicates that efficient gas exchange via the intra-rectal route may be possible by both g-EVA and I-EVA protocols at a therapeutic level.

In *Misgurnus anguillicaudatus*, the intestinal air-breathing function starts to develop at around 10 days after hatching. A recent RNA sequencing (RNA-seq) analysis of the different developmental stages of the posterior intestines of *M. anguillicaudatus* revealed the existence of gene signatures closely related to the acquisition of the intestinal air-breathing function, such as the upregulation of vascularization (*VEGFA*, *SPON1B*) and mucosal inflammation (*ANXA1*) and the downregulation of oxidative phosphorylation (*GDH*).<sup>9</sup> Similar gene expression changes in the mouse distal intestine were observed by evaluating the mouse homologs *Vegfa*, *Spon1*, *Anxa1*, and *Glud1* with g-EVA (Figure S1A).<sup>9</sup> Loaches normally use bronchial respiration in standard oxygenated environments, but under



**Table 3. Serum endotoxin titer after O<sub>2</sub>-PFD administration**

	Gelation time, min	Dilution rate	Titer of endotoxin, EU/mL
Distilled water	>60	1	<0.003
Control 1	40 ± 0.14	100	0.055 ± 0.064
Control 2	18 ± 0.28	10	0.10 ± 0.024
Control 3	10 ± 0.14	1	1.0 ± 0.060
Mouse 1	>60	10	LLOQ
Mouse 2	>60	10	LLOQ
Mouse 3	>60	10	LLOQ
Mouse 4	>60	10	LLOQ
Pig 1	>60	10	LLOQ
Pig 2	>60	10	LLOQ

LLOQ, lower limit of quantitation (0.003 EU/mL).

hypoxic environments, they switch the posterior part of their intestine to an accessory respiration site for survival. When living under prolonged hypoxia, loaches and other species convert their intestinal digestive functions to intestinal respiration by modifying transporter and vascularization genes, while also strengthening their antioxidant systems and immune defenses.<sup>16</sup> It is also possible that modified digestive functions such as diminished transporter activities by g-EVA or l-EVA would be a contributing factor for oxygenation as was seen in the loaches. Elucidating further physiologic features and molecular signatures will maximize efficient oxygenation in the gut.

The use of perfluorochemicals is encouraging toward clinical translation because numerous clinical studies with different delivery methods highlight safe and tolerable features in patients.<sup>11–13</sup> For example, when an emulsified form of perfluorochemicals was administered directly into the blood vessels or the airway, relatively modest side effects were reported, including the elevation of blood pressure and injury to organs.<sup>12,17–19</sup> The level of arterial oxygenation, if scaled for human application, is likely sufficient to alleviate patients with severe respiratory failure. The administration of 200–400 mL PFD to pigs weighing 10–20 kg improved PaO<sub>2</sub> by 13 mm Hg (from 57.2 ± 13.5 to 70.8 ± 6.22 mm Hg) and SaO<sub>2</sub> by 7% (from 84% to 91%).<sup>20</sup> Using the formula for O<sub>2</sub> content ( $\text{CaO}_2 = 1.34 \times \text{Hb} \times \text{SaO}_2 + 0.003 \times \text{PaO}_2$ ), 13.1 mL dissolved O<sub>2</sub> is calculated to be absorbed via enteral ventilation. Assuming a 60-kg patient has the same gas exchange efficiency by EVA, 38.6 mL O<sub>2</sub> delivery would result in an improvement in SaO<sub>2</sub> by 5% and in PaO<sub>2</sub> by 10–20 mm Hg. As PFD used in this study has an O<sub>2</sub> solubility of 50 mL/dL, exposure of an estimated 600–1,200 mL O<sub>2</sub>-PFD potentially provides lifesaving oxygenation, while there is additional room for improving gas exchange efficacy. It is also worth noting that a much lower amount is applied in l-EVA compared to the 1,800 mL (30 mL/kg) usage in total liquid ventilation via the lung. Given that no obvious toxicity events were identified in our preclinical study, at least during the short time course, the potential l-EVA indications would include patients who can benefit from immediate oxygenation supports such as bronchial asthma attacks, airway stenosis, neonatal asphyxia, and acute respiratory failure.

Interestingly, the arterial pressure of CO<sub>2</sub> tended to be decreased in the l-EVA group, presumably due to the excellent O<sub>2</sub> - and CO<sub>2</sub>-carrying capacity of perfluorochemicals (50 mL O<sub>2</sub>/dL and 160–210 mL CO<sub>2</sub>/dL, respectively), while the arterial pH did not change in our experiment. These results indicate that perfluorochemicals also act as an adsorbent for elevated CO<sub>2</sub>, indicating a need for future follow-up studies of gas exchange mechanisms.

Artificial respiratory support plays a vital role in the clinical management of respiratory failure due to severe illnesses such as pneumonia or acute respiratory distress syndrome (ARDS). Mechanical ventilation is the most commonly used short-term life support technique worldwide.<sup>21,22</sup> An artificial lung, called extracorporeal membrane oxygenation (ECMO), is an alternate approach for critically ill patients, used as a temporal palliative therapy.<sup>23</sup> However, in addition to concerns for iatrogenic complications such as ventilator-induced lung injury, bleeding and thrombosis, the recent severe acute respiratory syndrome-coronavirus-2 (SARS-CoV-2) pandemic has overwhelmed the clinical need for ventilators and ECMO, resulting in a critical shortage of available devices and endangering patients' lives worldwide. Without relying on such indwelling respiratory devices, EVA will offer a new paradigm as an adjunctive support to patients who are in critical need of respiratory supports for a short period.

### Limitations of study

A first limitation of our study includes unclear oxygenation mechanisms in the gut. Our collective data (increase in  $O_2$ , and decrease in  $CO_2$  without PFD absorption) support that there are diffusion-based gas exchange mechanisms, most likely at the rectal region, enhanced by the application of perfluorocarbon. These data warrant further mechanistic investigations. Second, we evaluated EVA efficacy primarily in asphyxia-like respiratory failure conditions. Further therapeutic investigations in severe pneumonia and ARDS models accompanied by systemic inflammation will broaden the clinical significance of our enteral ventilation approach. Third, despite remarkable short-term safety demonstrated in preclinical animal studies, it is critical to evaluate safety in humans before the approach is broadly applied in clinics.

### STAR★METHODS

Detailed methods are provided in the online version of this paper and include the following:

- KEY RESOURCES TABLE
- RESOURCE AVAILABILITY
  - Lead contact
  - Materials availability
  - Data and code availability
- EXPERIMENTAL MODEL AND SUBJECT DETAILS
  - Animals
- METHOD DETAILS
  - Intestinal gas ventilation in mice
  - Intestinal liquid ventilation in mice
  - Reversal of respiratory failure by g-EVA and l-EVA in mice
  - Reversal of respiratory failure by l-EVA in mice with pulse oximetry ( $SpO_2$ )
  - Reversal of respiratory failure by l-EVA in pigs
  - Behavioral analysis in mice
  - Hematoxylin eosin staining and quantification in mice
  - Immunohistochemical staining with Hypoxyprobe in mice
  - RT-qPCR analysis in mice
  - Perfluorodecalin measurements by gas chromatography mass spectrometry
  - Endotoxin (Lipopolysaccharide: LPS) analysis in mice and pigs
- QUANTIFICATION AND STATISTICAL ANALYSIS

## SUPPLEMENTAL INFORMATION

Supplemental information can be found online at <https://doi.org/10.1016/j.medj.2021.04.004>.

## ACKNOWLEDGMENTS

The authors would like to thank Hirofumi Nagai, Taiichi Mune, Ryo Miyata, Naoko Sekinami, Mitsuru Mizuno, Akiko Kinebuchi, and Vivian Hwa for their helpful discussions and technical assistance in the experiments. We also thank Asuka Kodaka for designing the graphical abstract. This work is funded by the Research Program on Emerging and Re-emerging Infectious Diseases, Research Projects on COVID-19 (JP20fk0108278, 20fk0108506h0001), from the Japan Agency for Medical Research and Development (AMED), to T.T.; Strategic Promotion for Practical Application of Innovative Medical Technology, Seeds A (A145), to T.T.; and KAKENHI 19K22657, to T.C.-Y. This research is partially supported by the AMED Translational Research Program; Strategic Promotion for Practical Application of Innovative Medical Technology (TR-SPRINT), to T.C.-Y.; and AMED JP18bm0704025h0001 (Program for Technological Innovation of Regenerative Medicine), to T.T. T.T. is a New York Stem Cell Foundation-Robertson Investigator.

## AUTHOR CONTRIBUTIONS

R.O. and T.T. designed the experiments; R.O., Y. Yoneyama, T.F.C.-Y., Y. Yokoyama, S.T., W.L.T., G.K., E.K., H.D., and T.T. wrote the manuscript; R.O., Y. Yoneyama, Y. Yokoyama, E.K., and T.T. performed the experiments; and T.F.C.-Y., K.W., and H.D. advised from a clinical point of view.

## DECLARATION OF INTERESTS

The authors declare no competing interests.

Received: October 22, 2020

Revised: February 10, 2021

Accepted: March 30, 2021

Published: May 14, 2021

## REFERENCES

1. Plaul, S.E., Barbeito, C.G., and Díaz, A.O. (2016). Histochemical differences along the intestine of *Corydoras paleatus* (Siluriformes: Callichthyidae). *Rev. Biol. Trop.* 64, 327–340.
2. Bickford, D., Iskandar, D., and Barlian, A. (2008). A lungless frog discovered on Borneo. *Curr. Biol.* 18, R374–R375.
3. Woods, H.A., Lane, S.J., Shishido, C., Tobalske, B.W., Arango, C.P., and Moran, A.L. (2017). Respiratory gut peristalsis by sea spiders. *Curr. Biol.* 27, R638–R639.
4. Barrie, H. (1959). Intragastric administration of oxygen. *Lancet* 1, 884–885.
5. James, L.S., Apgar, V.A., Burnard, E.D., and Moya, F. (1963). Intragastric oxygen and resuscitation of the newborn. *Acta Paediatr. (Stockh.)* 52, 245–251.
6. Virasoro, J.E., Pellerano, J.C., and Bertelli, S.A. (1959). Intragastric oxygen therapy: practical technic for administration in the newborn infant. *Sem. Med.* 114, 640–641.
7. Waller, H.K., and Morris, D. (1953). Resuscitation of the newborn with intragastric oxygen; Akerren's method. *Lancet* 265, 951–953.
8. de Boer, A.G., Moolenaar, F., de Leede, L.G., and Breimer, D.D. (1982). Rectal drug administration: clinical pharmacokinetic considerations. *Clin. Pharmacokinet.* 7, 285–311.
9. Luo, W., Cao, X., Xu, X., Huang, S., Liu, C., and Tomljanovic, T. (2016). Developmental transcriptome analysis and identification of genes involved in formation of intestinal air-breathing function of Dojo loach, *Misgurnus anguillicaudatus*. *Sci. Rep.* 6, 31845.
10. Zheng, L., Kelly, C.J., and Colgan, S.P. (2015). Physiologic hypoxia and oxygen homeostasis in the healthy intestine. A review in the theme: cellular responses to hypoxia. *Am. J. Physiol. Cell Physiol.* 309, C350–C360.
11. Sarkar, S., Paswan, A., and Prakas, S. (2014). Liquid ventilation. *Anesth. Essays Res.* 8, 277–282.
12. Yu, Q., Liu, K., Su, L., Xia, X., and Xu, X. (2014). Perfluorocarbon liquid: its application in vitreoretinal surgery and related ocular inflammation. *BioMed Res. Int.* 2014, 250323.
13. Khan, F., Singh, K., and Friedman, M.T. (2020). Artificial Blood: The History and Current Perspectives of Blood Substitutes. *Discoveries (Craiova)* 8, e104.
14. Leach, C.L., Greenspan, J.S., Rubenstein, S.D., Shaffer, T.H., Wolfson, M.R., Jackson, J.C., DeLemos, R., and Fuhrman, B.P. (1996). Partial liquid ventilation with perflubron in premature infants with severe respiratory distress syndrome. The LiquiVent Study Group. *N. Engl. J. Med.* 335, 761–767.
15. West, L., McIntosh, N., Gendler, S., Seymour, C., and Wisdom, C. (1986). Effects of intravenously infused Fluosol-DA 20% in rats. *Int. J. Radiat. Oncol. Biol. Phys.* 12, 1319–1323.

16. Huo, D., Sun, L., Ru, X., Zhang, L., Lin, C., Liu, S., Xin, X., and Yang, H. (2018). Impact of hypoxia stress on the physiological responses of sea cucumber *Apostichopus japonicus*: respiration, digestion, immunity and oxidative damage. *PeerJ* 6, e4651.
17. Chambers, D.C., Cherikh, W.S., Goldfarb, S.B., Hayes, D., Jr., Kucheryavaya, A.Y., Toll, A.E., Khush, K.K., Lewvey, B.J., Meiser, B., Rossano, J.W., and Stehlik, J.; International Society for Heart and Lung Transplantation (2018). The International Thoracic Organ Transplant Registry of the International Society for Heart and Lung Transplantation: Thirty-Fifth Adult Lung and Heart-Lung Transplant Report-2018; Focus Theme: Multiorgan Transplantation. *J. Heart Lung Transplant.* 37, 1169–1183.
18. Ferrari, R.S., Thomaz, L.D.G.R., Simoneti, L.E.L., Ulbrich, J.M., and Andrade, C.F. (2019). Effect of vaporized perfluorocarbon on oxidative stress during the cold ischemia phase of lung graft preservation. *J. Bras. Pneumol.* 45, e20170288.
19. Forgiarini Junior, L.A., Holand, A.R., Forgiarini, L.F., da Rosa, D.P., Marroni, N.A., Cardoso, P.F., and Andrade, C.F. (2013). Endobronchial perfluorocarbon reduces inflammatory activity before and after lung transplantation in an animal experimental model. *Mediators Inflamm.* 2013, 193484.
20. Serianni, R., Barash, J., Bentley, T., Sharma, P., Fontana, J.L., Via, D., Duhm, J., Bunger, R., and Mongan, P.D. (2003). Porcine-specific hemoglobin saturation measurements. *J. Appl. Physiol.* (1985) 94, 561–566.
21. Tobin, M., and Manthous, C. (2017). Mechanical Ventilation. *Am. J. Respir. Crit. Care Med.* 196, P3–P4.
22. Pham, T., Brochard, L.J., and Slutsky, A.S. (2017). Mechanical Ventilation: State of the Art. *Mayo Clin. Proc.* 92, 1382–1400.
23. Patel, B., Chatterjee, S., Davignon, S., and Herlihy, J.P. (2019). Extracorporeal membrane oxygenation as rescue therapy for severe hypoxemic respiratory failure. *J. Thorac. Dis.* 11 (Suppl 14), S1688–S1697.

## STAR★METHODS

### KEY RESOURCES TABLE

REAGENT or RESOURCE	SOURCE	IDENTIFIER
<b>Chemicals, peptides, and recombinant proteins</b>		
Basic fibroblast growth factor	Wakenyaku Co.,Ltd	Cas: 131094-16-1
Ketamine	Daiichi Sankyo Pharmaceutical	Cas: 1867-66-9
Xylazine	Bayer	Cas: 7361-61-7
Perfluorodecalin	Fujifilm Wako Pure Chemical or F2-Chemical inc.	Cas: 306-94-5
<b>Critical commercial assays</b>		
Hypoxyprome-1 Plus kit	Hypoxyprome	HP2-100
RNA later	QIAGEN	#76104
FastGene RNA Basic Kit	NIPPON Genetics	#FG-80050
ReverTra Ace qPCR Master Mix with gDNA remover	TOYOBO	#FSQ-301
THUNDERBIRD SYBR qPCR Mix	TOYOBO	#QPS-201
Limulus ES-II single test	Fujifilm Wako Pure Chemical Industries	#296-81501
<b>Software and algorithms</b>		
GraphPad software	Graphpad Software	<a href="https://www.graphpad.com/">https://www.graphpad.com/</a>

### RESOURCE AVAILABILITY

#### Lead contact

Further information and requests for resources and reagents should be directed to, and will be fulfilled by the Lead Contact, Takanori Takebe ([takanori.takebe@cchmc.org](mailto:takanori.takebe@cchmc.org)) or Eiji Kobayashi ([organfabri@keio.jp](mailto:organfabri@keio.jp)) for pig experiments.

#### Materials availability

This study did not generate any new materials or reagents.

#### Data and code availability

This study did not generate new codes.

### EXPERIMENTAL MODEL AND SUBJECT DETAILS

#### Animals

C57BL/6J mice were purchased from SLC (Shizuoka, Japan). Micro mini pigs were purchased from Fuji Micra Inc. (Shizuoka, Japan). These mice were bred in a pathogen-free environment with a 12-h light-dark cycle and free access to water and food. All animal care and experiments were carried out in accordance with institutional and national guidelines (Japanese Ministry of Education, Culture, Sports, Science and Technology). Studies using mice were approved by the Institutional Animal Care Committee (IACUC) of Kyoto University and Tokyo Medical and Dental University (Med Kyo 19583 and A2020-0140C). The pig experiments were carried out at the laboratory of Hamri Co., Ltd. (Ibaraki, Japan), which has been approved by the Association for the Assessment and Accreditation of Laboratory Animal Care (AAALAC) International. The experimental protocols (IB20044: 20–H054, IB20046: 20–H060) were approved by the IACUC of Hamri Co., Ltd.. All animals with mixed gender were randomly assigned to experimental groups.

## METHOD DETAILS

### Intestinal gas ventilation in mice

We designed an intestinal gas ventilation (g-EVA) system with the direct administration of pure oxygen into large intestine in mice. First, six intestinal abrasion methods were initially evaluated (see [Table S1](#)). Mice were randomly assigned to 8 groups ([Table S1](#)): Group 1, sham (n = 3); Group 2, non-abraded (n = 3); Group 3, oral administration of 2% dextran sulfate sodium (DSS) for 5 days (n = 5); Group 4, rectal administration of 2% DSS for 5 days (n = 5); Group 5, oral administration of 2% DSS for 5 days and basic fibroblast growth factor (bFGF) was subsequently injected once per rectum (n = 6); Group 6, mild mechanical abrasion (n = 10); Group 7, moderate mechanical abrasion (n = 10); and Group 8, severe mechanical abrasion (n = 5). For Groups 1–8, skin incision was performed to take blood samples under anesthesia with ketamine (80–100 mg/kg) and xylazine (10 mg/kg). We administered pure oxygen per large intestine in a 4 cm range into the intestine and estimated venous gas including pH, oxygen, carbon dioxide, base excess, bicarbonate ion and lactate levels in the inferior vena cava in Group 2–8. Venous gas was also analyzed for Group 1, and 3 days after bFGF injection in group 5. In the mechanical group, abrasion of the intestinal mucosa was performed under anesthesia (see [Table S1](#)) and was induced by mechanical brushing with an interdental brush for specified time and length of intestine. In group 9–11, we applied artificial ventilation (Tidal 500  $\mu$ l/time, respiratory rate 100–120 breaths /min, positive end-expiratory pressure 2 cmH<sub>2</sub>O). Mice were randomly assigned into 3 groups: Group 9, a sham group (n = 10); Group 10, a non-abraded intestinal gas ventilation group (non-abraded g-EVA group, n = 7); Group 11, a mucosal abraded intestinal gas ventilation group (moderate abrasion, g-EVA group, n = 11, [Video S1](#)).

### Intestinal liquid ventilation in mice

Clinically, it is difficult to thin the intestinal mucosa. Therefore, Intestinal liquid ventilation (l-EVA) system was developed with liquid perfluorochemicals (1–5). We randomly assigned the mice into 2 groups: sham group (Group 9, n = 10) and an intestinal liquid ventilation group (Group 12, n = 12). For intestinal liquid ventilation (l-EVA), we loaded PFD (Octadecafluorodecahydronaphthalen, Wako chemical, Osaka, Japan) with oxygen, by bubbling pure oxygen for 45 minutes. 1 mL of PFD was administered via mouse rectum, and 120 minutes later we analyzed the venous gas including pH, partial pressure of oxygen and carbon dioxide, the concentration of base excess and bicarbonate ion in the inferior vena cava at the level of right renal vein. In order to prevent intestinal perforation, O<sub>2</sub>-PFD was slowly introduced into the rectum over a period of several minutes. O<sub>2</sub>-loaded PFD was administered at room temperature.

### Reversal of respiratory failure by g-EVA and l-EVA in mice

For g-EVA experiments, the animals were randomly assigned into 2 groups ([Table S1](#)): Group 13, a non-intestinal ventilation group (sham group, n = 4); Group 14, intestinal gas ventilation with abrasion of the mucosa group (moderate abrasion, g-EVA group, n = 4). Skin and tracheal incisions under anesthesia and mechanical ventilation was performed as described above. For Group 14, pure oxygen was administered into the intestinal lumen. In addition, hypoxic oxygen (FiO<sub>2</sub> 0.10) was administered into the mice's airway 10 minutes after artificial ventilation and the arterial gas including pH, partial pressure of oxygen and carbon dioxide in the left ventricle of the heart estimated 10 minutes after the administration of the hypoxic oxygen. Survival experiments were conducted by FiO<sub>2</sub> 0.08 conditions as FiO<sub>2</sub> 0.10 is sublethal. The animals were randomly assigned into 3 groups ([Table S1](#)): Group 15, sham group (n = 3); Group 16, an intestinal gas ventilation group



(non-abraded g-EVA,  $n = 4$ ); Group 17, a mucosal abraded intestinal gas ventilation group (moderate abrasion, g-EVA,  $n = 4$ ). We compared the survival rate and the clinical characteristics including opacity of the eye, cardiac arrest, continuation of agonal respiration, arrest of mesenteric arterial pulse and skin pallor among Groups 15, 16, and 17 (Table S2). For I-EVA experiments, we randomly assigned the mice into 2 groups: sham group (Group 13,  $n = 4$ ), and an I-EVA group (Group 18,  $n = 4$ ; Group 19,  $n = 4$ ).  $O_2$ -PFD was given via mouse rectum as mentioned above, and 60 and 120 minutes later we analyzed the arterial gas including pH, partial pressure of oxygen and carbon dioxide in the left ventricle of the heart under hypoxic inhalation ( $FiO_2$  0.10, the inhalation time; 10 minutes).

### Reversal of respiratory failure by I-EVA in mice with pulse oximetry ( $SpO_2$ )

For I-EVA experiments, the animals were randomly assigned into 2 groups (Figure 2F): saline group (sham group,  $n = 2$ ); I-EVA group (therapy group,  $n = 3$ ). Skin and tracheal incisions under anesthesia and mechanical ventilation was performed as described above. Hypoxic oxygen ( $FiO_2$  0.10) was administered into the mice's airway 10 minutes after artificial ventilation. For therapy group,  $O_2$ -PFD was administered into the intestinal lumen after the  $SpO_2$  fell below 60%. Mice were subjected to continuous monitoring of oxygen saturation by pulse oximetry (MouseOx, Prime-tech Corp., Tokyo, Japan).

### Reversal of respiratory failure by I-EVA in pigs

Repeated  $O_2$ -PFD and  $O_2$ -saline administration group (Rep group:  $n = 4$ ) was established. All animals underwent operation under anesthesia with ketamine, xylazine as anesthetic induction. After tracheal intubation, we used isoflurane and oxygen as anesthetic maintenance. In addition, two tubes for drainage and injection of therapeutic agents were inserted into descending colon after abdominal middle incision. Respiratory failure under 90% of  $SpO_2$  was established to decrease respiratory frequency (non-lethal hypoventilation model). Perfluorodecalin (Fujifilm Wako Pure Chemical CO., Osaka, Japan) was used for perfluorochemicals.  $O_2$ -saline and  $O_2$ -PFD were produced by bubbling saline and PFD with pure oxygen for 30 minutes, respectively before administration. Next, 20–40 ml/kg of the oxygen-bubbling saline ( $O_2$ -saline), the oxygen-bubbling PFD ( $O_2$ -PFD) was administered into descending intestine with circulatory method in the Rep group. Equal volumes of  $O_2$ -saline and  $O_2$ -PFD administered at the timing of hypoxic manifestation.  $O_2$ -saline was administered once per pig, and  $O_2$ -PFD was repeated three times per pig. Re-administration of  $O_2$ -PFD was carried out when the increased  $SpO_2$  dropped to the pre-treatment level.  $O_2$ -PFD can be recycled after collection into an outlet bag (Argyle™ Dennis™ colorectal tube, CardinalHealth™, Tokyo, Japan) placed in the rectum of the pig. Blood pressure, peripheral arterial oxygen saturation ( $SpO_2$ ), endo tidal carbon dioxide ( $EtCO_2$ ) and arterial blood gas analysis were estimated during the experiments. We used iSTAT analyzer (Abbot Point of Care Inc. IL, USA) for arterial gas analysis. The clinical characteristics were assessed including respiratory rate, intra-operative death, skin pallor, peripheral coldness and intestinal edema between  $O_2$ -PFD and  $O_2$ -saline administration group (Table S3). Pathohistological findings of the descending colon, rectum, liver and spleen were analyzed (Figure S3). In the Rep group, A total of ten repeated doses of  $O_2$ -PFD were administered. Furthermore, liver function including aspartate transaminase (AST) and alanine aminotransferase (ALT) was measured before and after administration of  $O_2$ -PFD. DRI-CHEM NX500V (Fujifilm CO., Tokyo, Japan) was used to measure liver function.

### Behavioral analysis in mice

We analyzed the behavioral improvements of hypoxic mice treated with the I-EVA. The mobility of each mice was monitored by a set of 2 parameters from the fit ellipse: centroid position (x, y). We calculated the walking distance of mice with these parameters every 20 s in the sham and therapy group (n = 3, for both). In total, we observed the walking behavior of each mouse for 5 minutes. We used O<sub>2</sub>-labeled perfluorodecalin as described above in the therapy group and applied hypoxic inhalation (FiO<sub>2</sub> 0.10) 120 minutes after rectal injection (Figure 2B).

### Hematoxylin eosin staining and quantification in mice

Adult loaches, *Misgurnus anguillicaudatus* (average body length of approximately 15 cm), were purchased from Meito Suien Co., Ltd (Aichi, Japan). Intestines from C57BL/6J mice and adult loaches were analyzed. Mouse intestines were from a non-intestinal respiration group (Group 1, sham group), an intestinal respiration group (Group 2, non-abraded g-EVA group) and an intestinal respiration group with abrasion of the mucosa group (Group 7, abraded g-EVA group). In the loach, pathohistological analysis was performed on the posterior intestine reported to undergo intestinal respiration. Slides, prepared from mounted, formalin-fixed paraffin-embedded tissue, were stained with hematoxylin and eosin. Under high-power microscopy (400 ×, optical microscope), 20 randomly fields were selected and each parameter was scored in a blinded fashion. For slides from Group 7 samples, we estimated the distances between the intestinal lumen and muscularis mucosa at 5 random positions. Each slide was scored by 3 independent evaluators, including an experienced pathologist and a surgeon.

### Immunochemical staining with Hypoxyprobe in mice

Immunochemical analyses of the intestinal region undergoing intestinal respiration was performed using the Hypoxyprobe-1 kit (HP2-100, Hypoxyprobe, Inc., Burlington, MA) following the manufacturer's instructions (6). Briefly, Hypoxyprobe-1 solution was injected into the peritoneum of mice at a dosage of 60 mg/kg body weight. Sections of the intestine were fixed with 10% neutral-buffered formalin, underwent antigen retrieval (blocking solution, 20 minutes at 90°C), washed in PBST (PBS +0.1% Triton X-100), and exposed to FITC-conjugated anti-pimonidazole mouse monoclonal primary antibody for 60 minutes at room temperature. After further PBST washes, a peroxidase conjugated anti-FITC rabbit secondary antibody was applied, and visualized under an optical microscope BX 43 (Olympus Co. Ltd., Tokyo, Japan). As indicated, signal intensity of 10 mucosal epithelial cells adjacent to each intestinal villa were scored as negative cells (zero point), weakly positive cells (one point), or strongly positive cells (two points). 5 fields in total were evaluated and total points, calculated. Three evaluators, including an experienced pathologist and surgeon, independently scored each slide.

### RT-qPCR analysis in mice

To determine gene expression changes associated with moderate and severe mechanical abrasion of intestine, mice were sacrificed at 0 minutes, 20 minutes, 6 hours and 24 hours after abrasion of the intestinal mucosa (n = 12 per mechanical abrasion). The intestinal tissues were harvested and immediately stored in RNA later (-QIAGEN, Hilden, Germany). Total RNA from the tissues was extracted with Fast-Gene RNA Basic Kit (NIPPON Genetics Co., Ltd., Tokyo, Japan). First-strand cDNA was synthesized with ReverTra Ace qPCR Master Mix with gDNA Remover (TOYOBO, Osaka, Japan). Quantitative PCR was performed with THUNDERBIRD SYBR qPCR Mix (TOYOBO, Osaka, Japan) on a QuantStudio 3 real time PCR system (ThermoFisher Scientific, Tokyo, Japan). A standard curve was prepared for each

gene for relative quantification, and expression level of each gene was normalized to the Rn28s gene. Specific primers used were: *Vegfa*-F 5'-AGGCTGCTGTAACGATGAAG-3' and *Vegfa*-R 5'-TCTCCTATGTGCTGGCTTTG-3'; *Anxa1*-F 5'-CCAGCACTCCAGCTTTCTTT-3' and *Anxa1*-R 5'-TCCGAACGGGAGACCATAAT-3'; *Spon1*-F 5'-AGAGAACCAGGAGGGAGATAAG-3' and *Spon1*-R 5'-GCCACAGGACAGTTACTCATAAA-3'; *Glud1*-F 5'-TACCGTTTGGAGGTGCTAAAG-3' and *Glud1*-R 5'-CCATAGTGAACCTCCGTGTAAT-3'

#### Perfluorodecalin measurements by gas chromatography mass spectrometry

Three Crl:CD (SD) rats in each group were divided into three groups: the control group received saline at a dose of 1 mL/rat, and the medicated group received PFD (F2-chemical, inc) at a dose of 1 and 1.5 mL/rat, administered intrarectally six times daily at a dosing interval of approximately 1 hour and 20 minutes. Blood concentrations of PFD in rat whole blood were determined 0.5, 2, and 24 h after completion of the 1-h storage of the last dose using gas chromatography-mass spectrometry. The measurements were carried out at Sumika Chemical Analysis Center Co., Ltd. (Osaka, Japan).

#### Endotoxin (Lipopolysaccharide: LPS) analysis in mice and pigs

To evaluate serum endotoxin levels, the serum samples in mice were collected 120 min after O<sub>2</sub>-saline or O<sub>2</sub>-PFD administration (Control group: O<sub>2</sub>-saline, n = 1, therapy group: O<sub>2</sub>-PFD, n = 3). Endotoxin was measured by the turbidimetric method using the Limulus ES-II single test (Fujifilm Wako Pure Chemical Industries, Osaka, Japan) and a toxinometer ET-6000™ (Fujifilm Wako Pure Chemical Industries, Osaka, Japan) (7). Distilled water was used for negative control, and positive control was divided into three groups with Dilution rate of 100x, 10x, and 1x using Limulus ES-II Single Test Wako control standard. To evaluate serum endotoxin levels, the serum samples in pigs were collected after the last O<sub>2</sub>-PFD administration in the experiments in which respiratory failure was reversed by I-EVA (n = 3). The method for measuring endotoxin levels is the same for the mice.

#### QUANTIFICATION AND STATISTICAL ANALYSIS

Statistical analyses were performed using GraphPad software (San Diego, CA, USA). Survival rates were determined using the Kaplan-Meier method and differences between groups were tested using the log-rank test. The differences in venous or arterial gas among the sham and the g-EVA groups or I-EVA groups were each analyzed by the unpaired t test or ANOVA plus the Tukey post hoc test. The histological analysis (the distance between intestinal lumen and muscularis mucosae, the estimated score with hypoxyprobe) were each analyzed by the Wilcoxon signed rank test. The A p value less than 0.05 was considered statistically significant. All data are shown as a mean  $\pm$  standard deviation (SD).